

# **Gear-Shaped Micromixer for Synthesis of Silica Particles Utilizing**

## **Inertio-Elastic Flow Instability**

### *Supplementary Information*

Sun Ok Hong<sup>a</sup>, Ki-Su Park<sup>b</sup>, Dong-Yeong Kim<sup>b</sup>, Sung Sik Lee<sup>c, d\*</sup>, Chang-Soo Lee<sup>b\*</sup>, and Ju Min Kim<sup>a, e\*</sup>

<sup>a</sup>Department of Energy Systems Research, Ajou University, Suwon 16499, Republic of Korea

<sup>b</sup>Department of Chemical Engineering and Applied Chemistry, Chungnam National University, Daejeon 305-764, Republic of Korea

<sup>c</sup>Institute of Biochemistry, ETH Zürich, Zürich, CH-8093, Switzerland

<sup>d</sup>Scientific Center for Optical and Electron Microscopy (ScopeM), ETH Zürich, Zürich, CH-8093, Switzerland

<sup>e</sup>Department of Chemical Engineering, Ajou University, Suwon 16499, Republic of Korea

**(Last Updated: November 23, 2020)**

\*To whom correspondence should be addressed:

\*E-mail: [jumin@ajou.ac.kr](mailto:jumin@ajou.ac.kr) (J. M. Kim); [rhadum@cnu.ac.kr](mailto:rhadum@cnu.ac.kr) (C.-S. Lee); [leesu@ethz.ch](mailto:leesu@ethz.ch) (S. S. Lee)

## Newtonian flow dynamics in serpentine microchannels

We investigated inertial effects on the flow dynamics of Newtonian fluids in a serpentine microchannel. In this study,  $Re$  varied from 0.7 to 41.7, which corresponds to the flow rate range of  $0.2 \leq Q \leq 12$  ml/h. A secondary Dean flow normal to the mainstream develops along the curved streamline in Newtonian fluid flow, as centrifugal force became increasingly important with increasing flow rate<sup>1,2</sup>. To investigate the onset of secondary Dean flow, we visualized the Newtonian flow in a serpentine microchannel at various flow rates, using fluorescent microscopy. 17 wt% glycerol aqueous solutions with fluorescent dye and dye-free were injected through two inlets. They merged at the junction in the serpentine microchannel (Fig. 1(b)). At a low flow rate ( $Re < 5$ ), the inertial effect was not significant and the interface between the dye and dye-free streams was clearly apparent to the end of the channel (Fig. S2(a) and (b)). To investigate secondary flow in our microfluidic channel, we performed numerical simulations with commercial software (COMSOL Multiphysics®) using the same parameters as the experimental conditions. (Fig. S3). At a low flow rate ( $Re < 5$ ), no lateral motion was predicted so that the strength of the secondary flow ( $S$ ) was nearly 0, where  $S$  is defined by  $S = \sqrt{u_y^2 + u_z^2}$  and  $u_y$  and  $u_z$  are the velocity components in the horizontal and vertical directions in the channel cross-section, respectively.  $S_{\max}$  is the maximum value of  $S$  in the cross-section. As  $Re$  increased above 5, the predicted streamlines exhibited clear outward fluid motion normal to the mainstream along the curved channel (Fig. S3(a) and the inset of S3(b)). Experimentally, we observed the outward motion by secondary flow generation at  $Re = 20.8$  ( $Q = 6$  ml/h) (Fig. S2(c) and (d), designated with red arrows), while no lateral motion was observed up to  $Re = 3.5$  ( $Q = 1$  ml/h). We note that the convection effect of secondary flow in the Newtonian flow mainly distorted the boundary of the fluid streams; however, this did not result in mixing of the streams until the end of the mixing zone (Fig. S2(d)).

**Table S1.** Size analysis data for the nanoparticles synthesized in both viscoelastic and Newtonian fluids. Standard deviation (SD), average size (AVG) and coefficient of variance ( $\equiv$ SD/AVG) for each independent experimental run are presented.

<b>Viscoelastic</b>	#1	#2	#3	#4	#5
SD (nm)	23.9	29.8	30.3	34.0	29.5
AVG (nm)	338.7	346.2	353.3	397.0	343.1
CV (%)	7.1	8.6	8.6	8.6	8.6

<b>Newtonian</b>	#1	#2	#3
SD (nm)	79.7	80.5	77.5
AVG (nm)	376.9	359.8	374.1
CV (%)	21.1	22.4	20.7

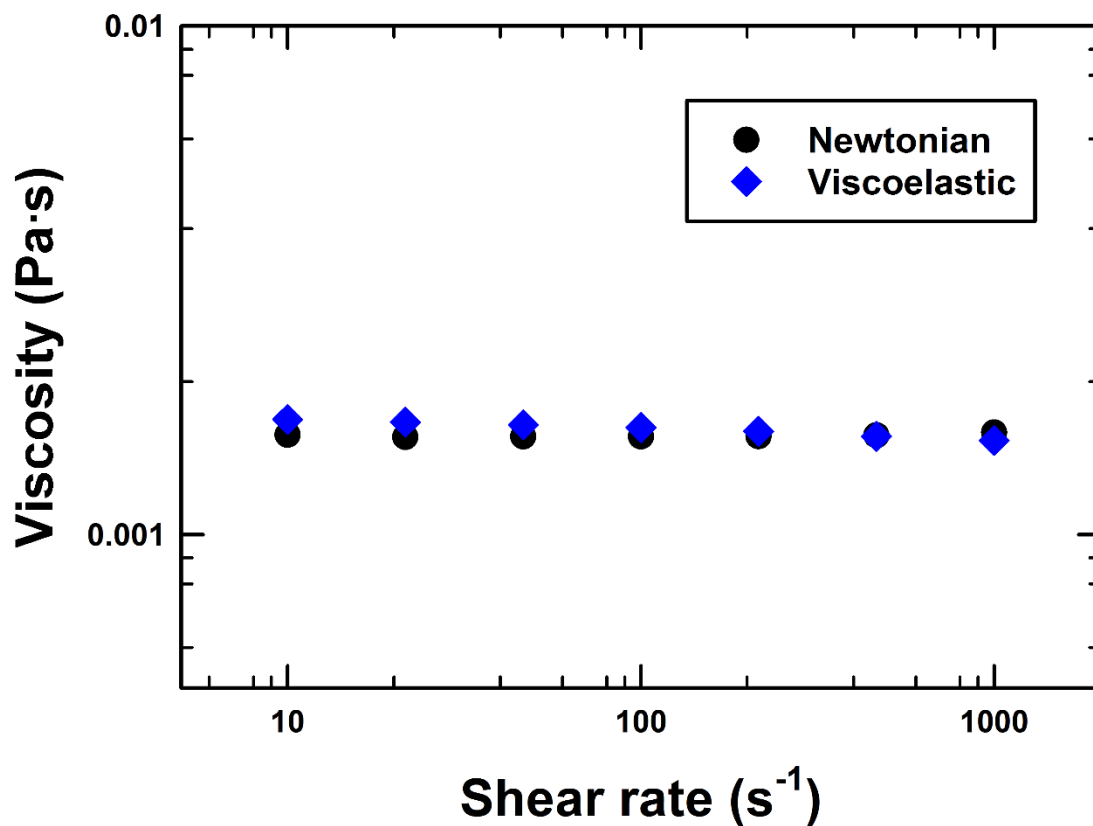


**Fig. S1. Steady shear viscosities of Newtonian and viscoelastic solutions as a function of shear rate.** The Newtonian solution was 17% glycerol solution in deionized (DI) water, and the viscoelastic solution was 500 ppm poly (ethylene oxide) (PEO; MW = 2 MDa) solution in DI water. Steady shear viscosity was measured with a stress-controlled rheometer (AR-G2, TA Instruments) with a cone-and-plate geometry (60 mm, 1°) at 20 °C. The shear viscosities of both Newtonian and viscoelastic fluids are nearly constant at 1.6 mPa s, irrespective of shear rate. The shear viscosity measurements were conducted 3 times for each solution, and the error bars were not denoted since they are all within the symbol sizes.

## Newtonian fluid in a serpentine microchannel

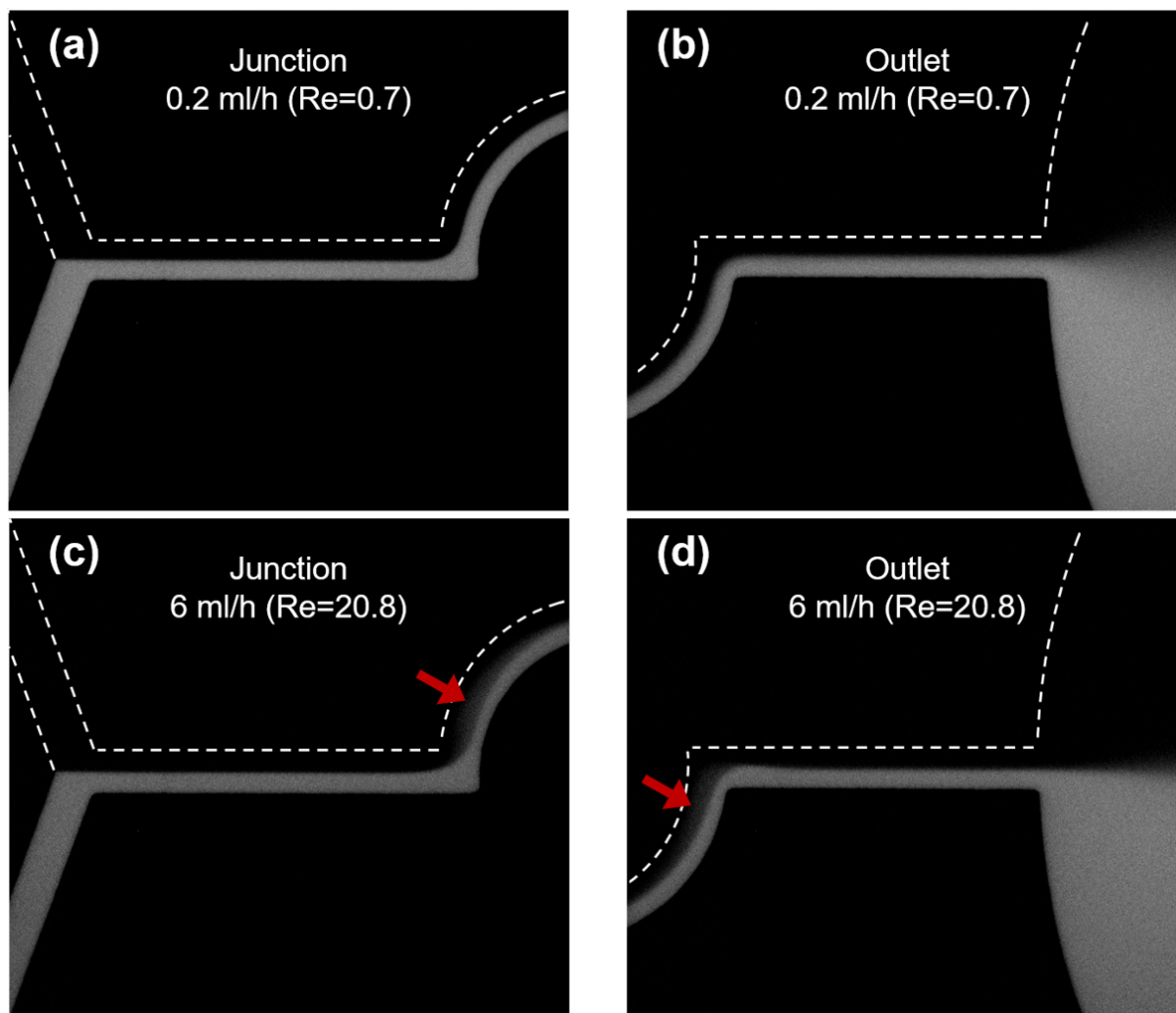


**Fig. S2. Fluorescent images of Newtonian solution in a serpentine microchannel at both junction and outlet regions.** (a) and (b) before the critical flow rate of the secondary flow generation [total flow rate: 0.2 ml/h ( $Re = 0.7$ )]. (c) and (d) after the onset flow rate of secondary flow developed along the curved streamlines (total flow rate: 6 ml/h ( $Re = 20.8$ )). The overall flow direction is from left to right. White dashed lines indicate the channel walls of the dye-free streams. Red arrows in (c) and (d) denote the distortion of boundary between dyed and dye-free streams arising from the lateral fluid motion by the secondary Dean flow.

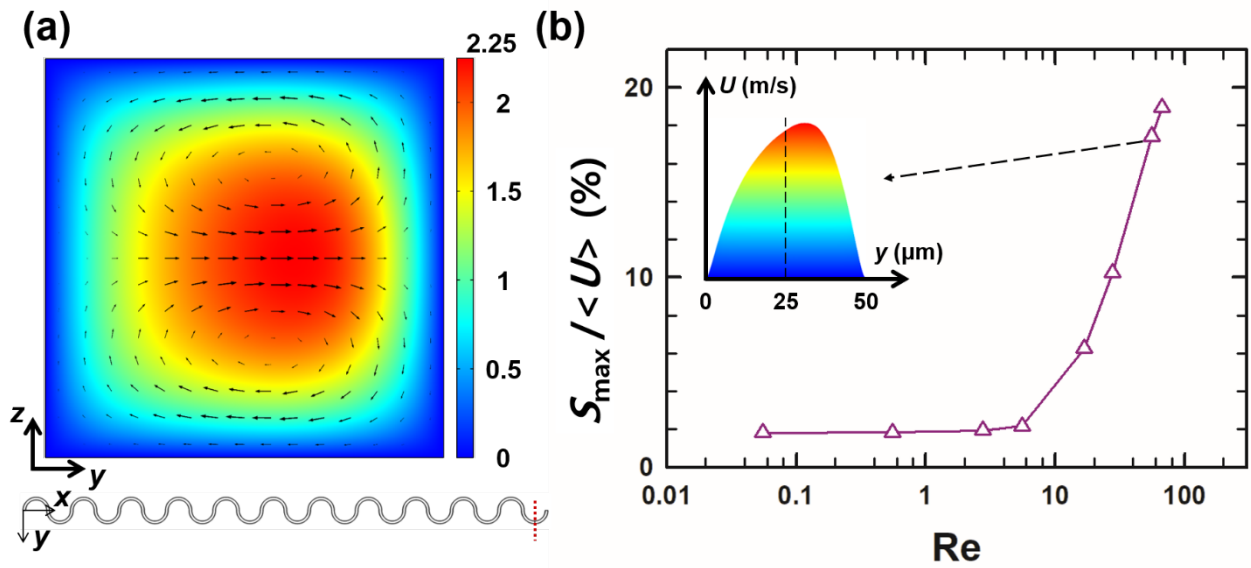


**Fig. S3. Numerical simulation results of a Newtonian fluid in a serpentine microchannel.** We numerically calculated the velocity field of Newtonian fluid using finite element analysis (COMSOL Multiphysics®). Stationary laminar flow model was chosen to predict the fluid motion with isothermal conditions (20 °C). Both width and height in the channel cross-section ( $yz$ -plane) were 50  $\mu\text{m}$ . **(a)** Velocity field in the last half-ring of the serpentine channel: cross-sectional view ( $Re = 55.6$ ) (refer to the last half-ring denoted with a red dashed line in the bottom channel schematic diagram). Arrows denote the vector field by the secondary flow and the length of arrow vectors is proportional to the strength of the secondary flow ( $S = \sqrt{u_y^2 + u_z^2}$ ). Colored background represents the velocity magnitude of the main stream ( $U$ ; unit: m/s). **(b)** Normalized maximum secondary flow strength,  $S_{\text{max}}/\langle U \rangle$ , is plotted as a function of  $Re$ .  $S_{\text{max}}$  and  $\langle U \rangle$  denote the maximum  $S$  value and the average streamwise velocity in the channel cross-section, respectively. Inset is the velocity magnitude ( $U$ ) at the last half ring along  $y$ -coordinate ( $Re = 55.6$  and  $z = 25 \mu\text{m}$ ).

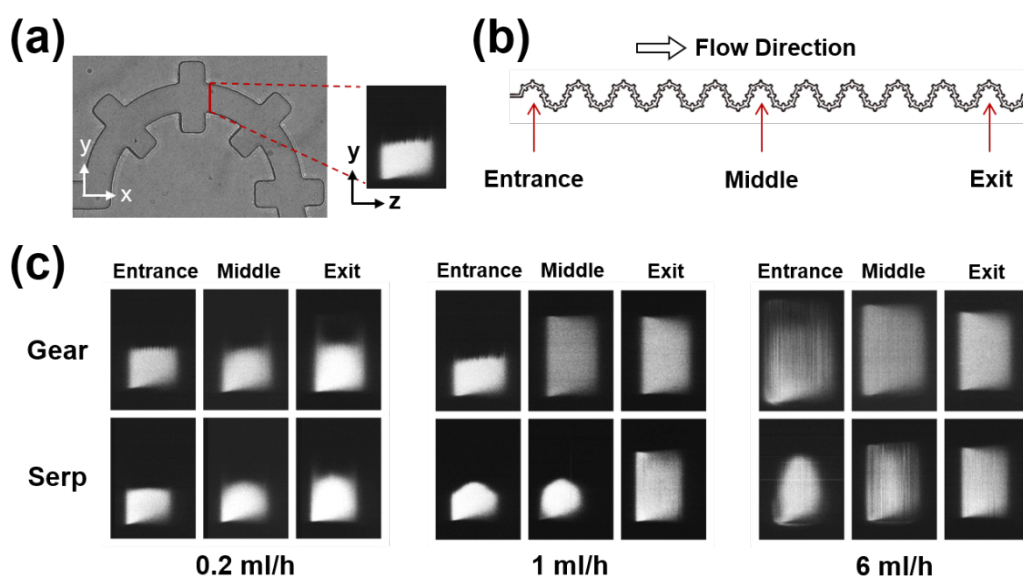


**Fig. S4. Mixing performance in the cross-sectional area.** We acquired z-stack fluorescent images at multiple points of the serpentine channels w/ or w/o side-channels using Nipkow spinning disk confocal system (CSU-W1-T2, Yokogawa Electric Corporation). Two solutions with fluorescent dye (500 ppm FITCD), and dye-free were injected through two inlets. By using orthogonal view tool in ImageJ (NIH), z-stack images in the  $zy$ -plane were converted to the  $xy$ -plane. **(a)** Bright field image shows the location where the images were acquired, and the fluorescence image at the right-hand side is the cross-sectional view at the same location. **(b)** We chose 3 different locations at the mixing zone with Entrance, Middle and Exit of the mixing zone to compare the progress of the mixing. The same three locations were chosen for both gear-shaped and traditional serpentine microchannels. **(c)** Comparison of the progress in mixing in both microchannels according to location in the mixing zone and the flow rate. At the low flow rate of 0.2 ml/h, mixing did not occur in either the gear-shaped or traditional serpentine microchannels. When the flow rate increased to 1 ml/h, mixing occurred before the middle of the mixing zone in the gear-shaped microchannel whereas mixing occurred only after the middle of the mixing zone in the traditional serpentine channel. At the high flow rate of 12 ml/h, mixing was observed after the middle of the mixing zone for both gear-shaped and traditional serpentine microchannels.

#### References in Supplementary Information

1. W. R. Dean, *Philos. Mag.*, 1927, **4**, 208-223.
2. W. R. Dean, *Philos. Mag.*, 1928, **5**, 673-695.

**Supplementary Movie SM1.** Sequential streak images in viscoelastic solution (500 ppm PEO (2 MDa) aqueous solution) in a gear-shaped microchannel at the flow rate of  $Q = 1$  ml/h [ $Re = 3.5$  and  $Wi = 1.5$  ( $Wi_{mod} = 0.9$ )]: the images were acquired at 10 frames per second (fps) with an exposure time of 50 msec and played at 15 fps. Red fluorescent microspheres of 500 nm diameter (Thermo Fisher Scientific) were added into the viscoelastic solution at the concentration of 0.001 wt%. 0.02 wt% Tween20 (Sigma-Aldrich) was also added to the solution to minimize the adhesion of particles onto the channel walls. Flow field was illuminated with a metal-halide lamp (Lumen 200, Prior) and observed on an inverted microscope (IX71, Olympus) equipped with an10X objective lens and a CCD camera (DMK 23u445, The Imaging Source).